ELSEVIER

Journal of Photochemistry and Photobiology A: Chemistry 141 (2001) 201–207

Journal of Photochemistry and Photobiology A:Chemistry

www.elsevier.nl/locate/jphotochem

Photodegradation mechanism of heterocyclic two-nitrogen containing compounds in aqueous TiO_2 dispersions by computer simulation

Satoshi Horikoshi, Hisao Hidaka*

Frontier Research Center for the Global Environment Protection (EPFC), Meisei University, 2-1-1 Hodokubo, Hino, Tokyo 191-8506, Japan

Received 13 February 2001; received in revised form 6 April 2001; accepted 10 April 2001

Abstract

The photocatalytic degradation of six-membered heteroaromatics (pyridazine, pyrimidine and pyrazine) in aqueous TiO_2 suspension was investigated. The initial mechanistic sequence(s) in the TiO_2-photocatalyzed oxidation of the constituent heterorings was predicted theoretically by molecular orbital (MO) calculations such as frontier electron densities and point charges on all the atoms. The cleavage of the heterocyclic moiety was examined by UV–VIS spectroscopy. The evolution of N_2 and CO_2 gas was determined by gas chromatography. The formation of NH_4^+ and NO_3^- ions was assessed by ion-HPLC, and that of carboxylic acid intermediates by HPLC. The disappearance of six-membered heteroaromatics and the formation of intermediates were observed by LC-MSD. The heterorings containing an N=N fragment lead to the evolution of N_2 gas, and those containing a C–N=C fragment lead to the generation of a large amount of NH_4^+ ions and a minor amount of NO_3^- ions. The photodegradation of these heteroaromatics is closely related to the position of the nitrogen in the heterorings. The mechanism of the photodecomposition of the heterocyclic aromatics was revealed through comparison of experimental data with the analytical simulation.

Keywords: Photooxidation; Photodegradation; Titanium dioxide; Pyridazine; Pyrimidine; Pyrazine

1. Introduction

Photocatalytic decomposition on TiO_2 semiconductors has been found to be an effective strong oxidation in advanced oxidation technology. The photomineralization of organic compounds containing heteroatoms has recently attracted attention. Phosphorus, sulfur and chlorine in heterocyclic compounds can be photomineralized to the inorganic ion species PO_4^{3-} [1–6], SO_4^{2-} [3,7] and Cl^- [8–14], respectively. Most nitrogen compounds can be converted photocatalytically into both ammonium and nitrate ions [15–19]. It is very difficult to identify the intermediate degraded products in the photocatalytic degradation of nitrogen-containing materials. The detailed mechanism of the formation of NH_4^+ and NO_3^- ions has not been elucidated until now. The evolution of N_2 gas in the photooxidation of N-containing compounds is better established than that of NH_4^+ and NO_3^- ions. The dependence of photooxidation on the chemical structure of heterorings with two nitrogen atoms has not yet been revealed.

We discuss in the following three aspects: (i) the photodegradation time course for different positions of the two nitrogen atoms in six-membered heteroring compounds; (ii) the initial photooxidation reaction on the TiO_2 surface; and (iii) comparison of computer simulation with the experimental data for the photodegradation.

2. Experimental section

2.1. Chemicals and reagents

The six-membered heterocyclic compounds of pyridazine (OP: *o*-$C_4H_4N_2$), pyrimidine (MP: *m*-$C_4H_4N_2$) and pyrazine (PP: *p*-$C_4H_4N_2$) having the same molecular weight 80.1 were supplied by Wako Pure Chem. Co. The chemical structure is shown below (the atom numbers are used in the molecular orbital (MO) calculations). The titanium dioxide photocatalyst was Degussa P25 (particle size, 20–30 nm by TEM microscopy; 83% anatase and 17% rutile determined by X-ray diffraction; surface area, 53 $m^2\,g^{-1}$ by the BET surface area measurement).

* Corresponding author. Fax: +81-42-599-7785.
E-mail address: hidaka@epfc.meisei-u.ac.jp (H. Hidaka).

1010-6030/01/$ – see front matter
PII: S1010-6030(01)00447-6

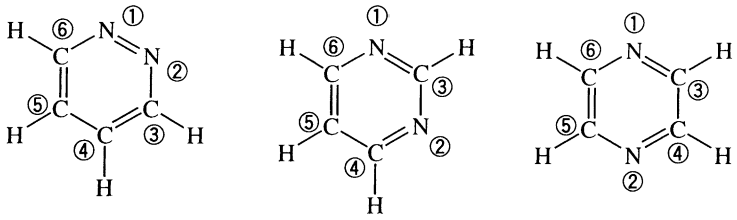

Pyridazine (OP) Pyrimidine (MP) Pyrazine (PP)

2.2. Photodegradation procedures and analytical methods

Aqueous solutions (1 mM, 50 ml) of the three chemicals were placed in the presence of TiO_2 powder (100 mg) in a 124 ml Pyrex vessel. The atmosphere in the photoreactor cell was purged with oxygen gas and the TiO_2 dispersion was then supersonicated. Irradiation of the dispersions was carried out with a 75 W mercury lamp, delivering 1.46 mW cm^{-2} in the wavelength range 310–400 nm (maximum emission at $\lambda = 360$ nm).

The ring opening of the cyclic compounds analyzed with a JASCO V-560 UV–VIS spectrophotometer. The concentration of ammonium and nitrate ions was assayed with a JASCO liquid chromatograph (HPLC) equipped with a CD-5 conductivity detector and either a Y-521 cation column or an I-524 anion column. The temporal evolution of N_2 and CO_2 was monitored by gas chromatography with an Ookura Riken chromatograph (model 802; TCD detection) through both a molecular sieve 5A (N_2 gas) and a Porapack Q column (CO_2 gas) with helium carrier gas. The formation of carboxylic acid intermediates for the photooxidation of samples was analyzed with a JASCO liquid chromatograph (HPLC) containing bromothymol blue (BTB), with a UV-detector for 445 nm and a KC-811 column. The generation of intermediates in the photodegradation of the six-membered cyclic compounds was determined with a Hewlett-Packard (HP) LC-MSD (electrospray ionization: EPA-AIC) in the mixed eluent of methanol and H_2O (1:1) equipped with an Agilent Eclipse XDB-C8 column.

2.3. Computer simulations

The computer simulation system used with a CAChe Worksystem version 3.2 (Fujitsu Co., Ltd.) was implemented on an Intel P-III and Windows 2000 system. The UV–VIS electronic transitions were calculated with ZINDO using INDO/1 parameters after geometrical optimization with augmented MM3 and MOPAC/PM3. The frontier electron density for radical attack and the point charge in the heteroaromatics were also calculated by a MOPAC/PM3 wavefunction. A geometrical configuration was determined by pre-optimization calculation in the mechanics using augmented MM3, followed by geometrically optimized calculation in MOPAC using PM3 parameters and the solvation effects in water was also simulated by COSMO [20–22].

3. Results and discussion

The photocleavage of six-membered heterorings is illustrated in Fig. 1. Three UV-absorption peaks for three homologues of OP, MP and PP were observed at 201, 246 and 300 nm, respectively.

The UV-absorption of OP at 246 and 300 nm decreased gradually with initial UV-irradiation time. The UV-absorption signal of OP at 201 nm started to disappear after 3 h illumination. However, the absorbance of MP and PP at 201 nm barely decreased after UV-illumination of 10 h. The UV-spectral patterns corresponding to a chemical structure were determined by ZINDO simulation. The position of chemical structure for the UV-absorption at 201 nm in each homolog was due to the N^1–C^6 and N^2–C^3 fragments in OP, the C^3 and C^5 atoms in MP, and the N^1 and

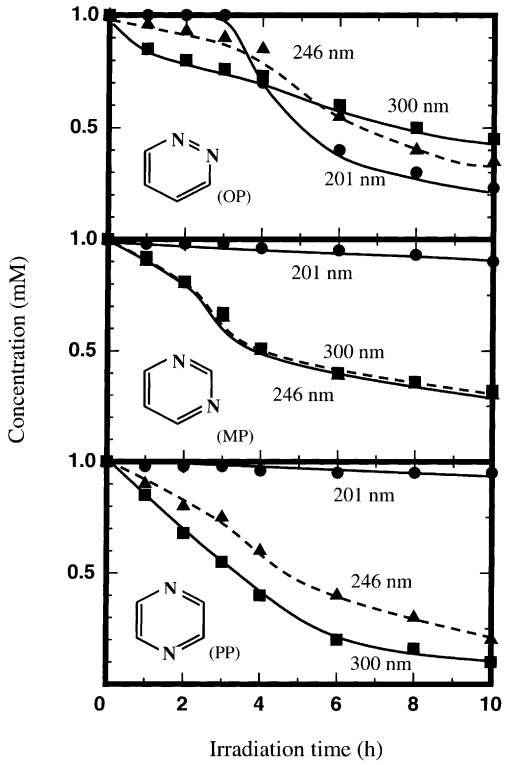

Fig. 1. Temporal photodegradation of pyridazine (OP), pyrimidine (MP) and pyrazine (PP) in the presence of TiO_2 (100 mg) under UV-illumination.

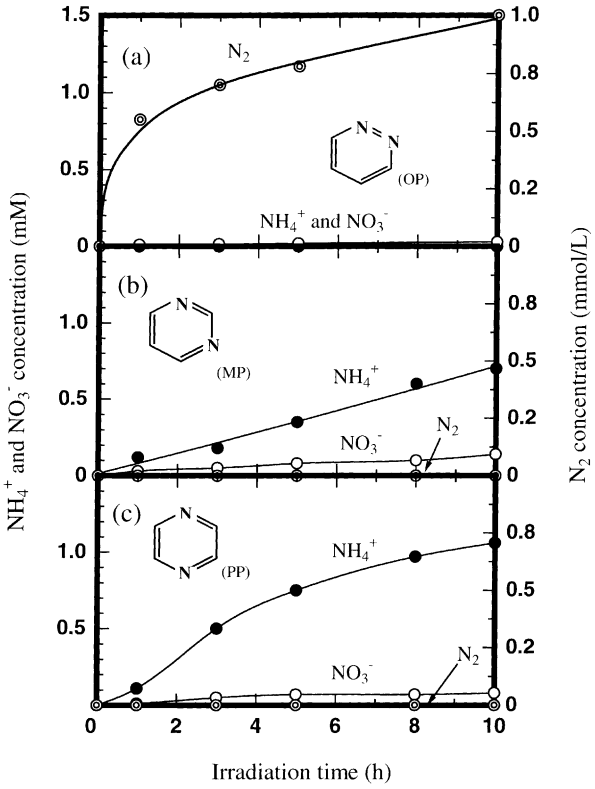

Fig. 2. Formation of NH_4^+ and NO_3^- ions, and evolution of N_2 gas in the photodecomposition of pyridazine (OP), pyrimidine (MP) and pyrazine (PP).

N^2 atoms in PP (see the atom numbers in the structures). The experimental results and simulations of UV-absorption enabled the initial photocleavage for each compound to be inferred. The initial photodegradation of OP involved bonds to carbon atoms, and reached the nitrogen and carbon atoms in the heteroring after illumination for 3 h. MP was photodecomposed at the N–C position. The photodecomposition of PP happened for the four carbon atoms in all UV-irradiation times.

The formation of NH_4^+ and NO_3^- ions, and N_2 gas in the photomineralization of the two nitrogen atoms, is shown in Fig. 2. No formation of NH_4^+ and NO_3^- ions in the photodegradation of OP was recognized even after UV-illumination for 10 h, but N_2 gas (about 1 mmol/l) was generated. The generation of N_2 gas was due to the scission of the C–N bonds resulting in the disappearance of UV-absorption at 201 nm after 3 h (see Fig. 1). The photomineralization of MP resulted in the predominant formation of NH_4^+ ions and a slight amount of NO_3^- (in the ratio, 5:1). The photomineralization of nitrogen atoms in PP was characterized by a ca. 12:1 ratio of NH_4^+ to NO_3^- ions after illumination of 10 h. The final photooxidized product for the heteroring containing N=N was N_2 gas, and the photooxidation of the C–N=C fragment in the heteroring yielded both NH_4^+ and NO_3^- ions, the amount of NH_4^+ ion being larger than that of NO_3^-.

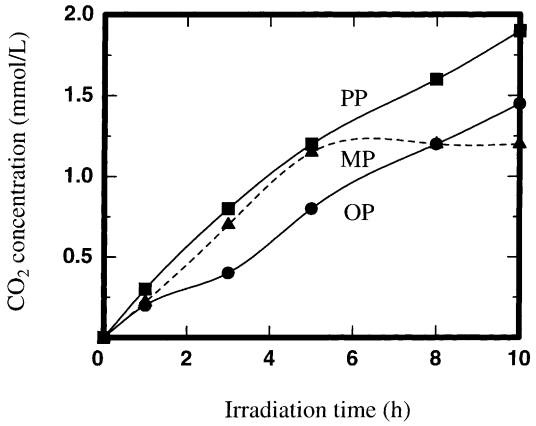

Fig. 3. Evolution of CO_2 gas in the photooxidation of pyridazine (OP), pyrimidine (MP) and pyrazine (PP).

The evolution of CO_2 gas is depicted in Fig. 3. The evolution of CO_2 gas in the photomineralization of the four carbon atoms in OP, MP and PP followed the order of PP $\geq$ MP $>$ OP under UV-illumination for 3 h, and it followed the order of PP $>$ OP $>$ MP after 10 h illumination. The photomineralization yields and the photodegradation rates with respect to two nitrogen atoms versus four carbon atoms are listed in Table 1. The photomineralization yield of the two nitrogen atoms in OP was seven times for that of the carbon atoms, and is considered to be rapidly photodegraded. The corresponding ratio for PP was 1.4, but the photomineralization yield of nitrogen atoms in MP was only 0.7 times that for carbon atoms. The photomineralization yield ratios for nitrogen atoms versus carbon atoms of each heteroring compound followed the order OP $\gg$ PP $>$ MP after illumination for 3 h, changing to OP $>$ MP $\geq$ PP at 10 h of illumination. The photooxidation of MP gave priority to carbon atoms for irradiation time of 3 h.

The formation of carboxylic acids in the degradation of OP, MP and PP is shown in Fig. 4(a)–(c), respectively. The carboxylic acid intermediates were formed by opening of the heterorings, and the further photooxidation of the carboxylic acids resulted in the evolution of CO_2 gas.

The initial intermediate formed from OP was propanoic acid, which reached the maximum peak at 1 h whereas the maximum amounts of formic and acetic acids were generated upon illumination of 2 h. The formation of formic and acetic acids was expected from the photooxidation of propanoic acid. No butanoic acid ($CH_3CH_2CH_2COOH$), containing four carbon atoms, formed during the photodegradation of OP. The initial photocleavage of the C=C bond was more preferred to that of the N–C bond since there was no change in UV-absorption at 201 nm for UV-illumination of up to 3 h. Propanoic acid, formic acid and tiny amount of acetic acid were continually generated. The intermediates produced in the photodegradation of MP were propanoic acid and acetic acid after 1 h irradiation. The predominant product in the photodecomposition of MP

Table 1
The photomineralization yields of pyridazine (OP), pyrimidine (MP) and pyrazine (PP)

	Photomineralization yields (%)								Photodegradation ratios of N vs. C $[(N_2 + NH_4^+ + NO_3^-)/CO_2]$	
	UV-irradiation of 3 h				UV-irradiation of 10 h				3 h	10 h
	N_2	CO_2	NH_4^+	NO_3^-	N_2	CO_2	NH_4^+	NO_3^-		
OP	70	10	0	0	100	36	0	0	7.0	2.8
MP	0	18	9	3	0	30	35	7	0.7	1.4
PP	0	20	25	3	0	48	53	4	1.4	1.2

was acetic acid. The initial cleavage in MP was of the C–N or C=N bonds, followed by the competitive formation of propanoic acid and acetic acid. A small amount of formic acid was formed after UV-illumination. The initial production of acetic acid was detected during the photodegradation of PP after illumination of 1 h. Formic acid was sparing by generated after further UV-irradiation.

Analysis of the initial adsorption on the TiO_2 surface and/or the photoactive site of the chemical structure was very difficult in the high-speed photoreaction. The negative charge in the chemical structure was attracted to the positively charged TiO_2 surface. The surface of the TiO_2 particles is charged positively in aqueous solutions below pH 6.3, changing to $=Ti–OH_2^+$ positive surface from =Ti–OH neutral surface. The pH value of each solution changed from ca. 4.8 to 5.4 during irradiation. Accordingly, the calculated negative charge in the heterorings indicated that at the beginning of the degradation the heteroring was attracted onto the TiO_2 surface. The reaction was initiated with the attack of $^\bullet$OH radicals from the TiO_2/OH^- (H_2O) interface formed by positive holes (h^+) after adsorption of the heterorings on the TiO_2 surface. The attack of $^\bullet$OH radicals led to a moiety of high frontier electron density of TiO_2. The calculation of the frontier electron density of the positions attacked by the $^\bullet$OH radical and the partial charges was accomplished by the MOPAC system (see Table 2). Atom numbers are seen on the chemical structures in the experimental section. The lifetime of the DMPO-OH adduct of an $^\bullet$OH radical on the TiO_2 surface with DMPO as the spin-trap agent was about 30 s according to ESR measurements, which was too short to pursue for the photodegradation pathway. As the distance between a negatively charged atom and an atom having a higher frontier electron density gets closer, the rate of photodegradation increases.

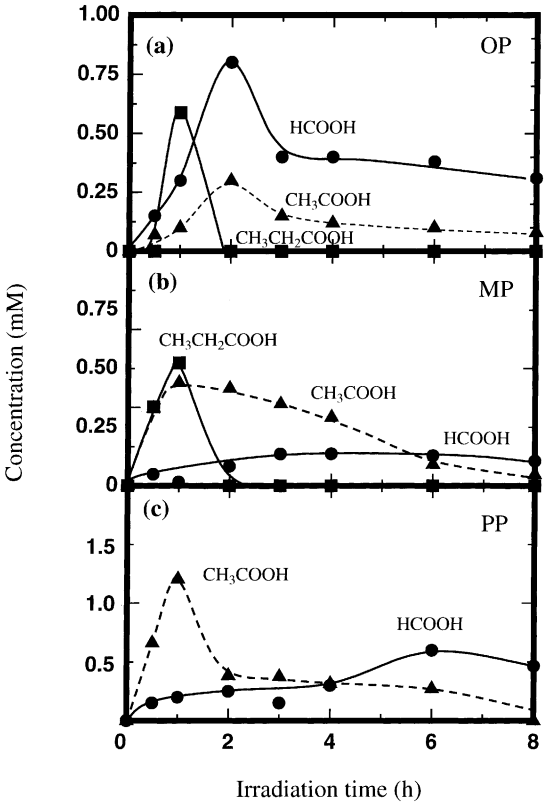

Fig. 4. Formation of carboxylic acid intermediates in the photooxidation of pyridazine (OP), pyrimidine (MP) and pyrazine (PP).

The atoms having the most negative charge in OP, MP and PP were all N^1 or N^2 atoms. However, the highest frontier electron densities of each heteroring were different. The richest frontier electron densities in OP were the C^3 and C^6 of the two C–N groups, which were therefore, susceptible to attack by $^\bullet$OH radicals. The nitrogen atoms were preferentially attracted onto the TiO_2 surfaces, hence the nitrogen atoms were photomineralized early in comparison with the carbon atoms. The frontier electron density of the C^5 atom of MP was larger than those of the other atoms, and those of the four carbon atoms of PP were higher than those of the

Table 2
Calculated point charges and frontier electron densities for pyridazine (OP), pyrimidine (MP) and pyrazine (PP) using the MOPAC method from the CAChe system

Atom	Point charge			Frontier electron density		
	OP	MP	PP	OP	MP	PP
N^1	−0.219	−0.390	−0.349	0.305	0.239	0.188
N^2	−0.218	−0.390	−0.349	0.304	0.238	0.188
C^3	0.099	0.260	0.099	0.390	0.376	0.401
C^4	−0.024	0.133	0.099	0.301	0.313	0.405
C^5	−0.024	−0.062	0.099	0.297	0.512	0.399
C^6	0.099	0.134	0.099	0.390	0.311	0.404

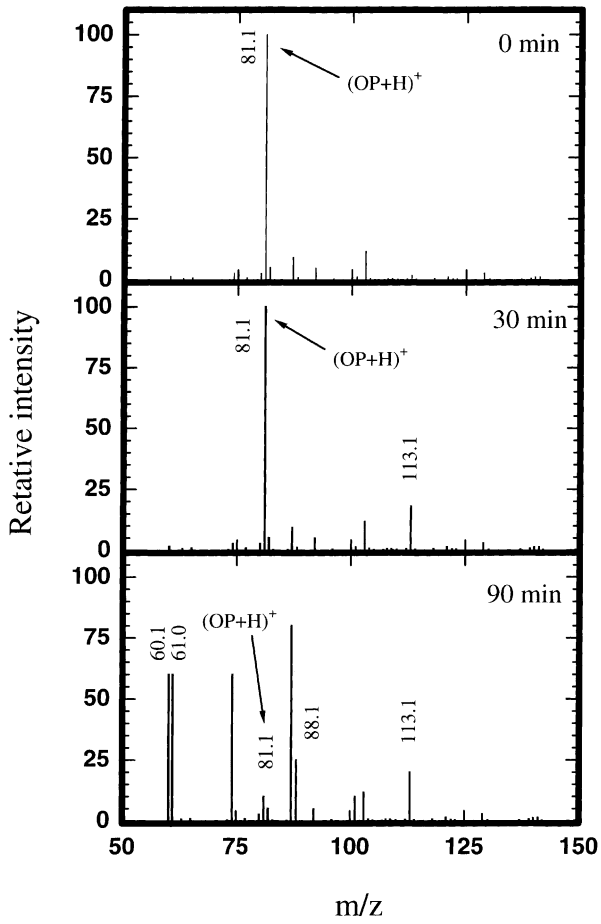

Fig. 5. Positive ion ESI mass spectrum in the photodecomposition of pyridazine (OP).

two nitrogen atoms. The actual product of the initial photodecomposition is determined by this distance.

The detection of intermediates in the photodegradation of six-membered heterorings was analyzed by HPLC/EPA mass spectrometry. Many intermediates were formed during the photodegradation of the heterorings, indicating competitive photodegradation between the heteroring (or the intermediates and) TiO_2 photocatalyst. The assignment of the photooxidation mechanism was usefully assisted by the characteristic data for increasing UV-irradiation time. The characteristic intermediates for OP corresponded to the both positive (cationic compounds: [material $+ H^+$]) and negative (anionic compounds: [material $- H^+$]) materials. The initial peak (81.1 *m/z*: OP+H) of OP (which has a molecular weight of 80) could hardly be observed after UV-illumination of 90 min (Fig. 5). The peak of 113.1 *m/z* was formed after irradiation for 30 and 90 min. The chemical structure of 113.1 *m/z* was attributable to HOC–N=N–CH=CH–COH, which was generated from the scission of the double bond (–C=C–). The photodegradation was correlated to the disappearance of UV-absorption and the MO simulation. Signal at 61.0 and 88.1 *m/z* in the photodecomposition of OP were discerned in the MS spectra after illumination of 90 min, and these new peaks were the expected intermediates of CH_3COOH and CH_2OH–CH=N–CHO. The formation of CH_2OH–CH=N–CHO from the scission of the N–C bond in the competitive photodecomposition of OP on TiO_2 surface was slower than the generation of CHO–N=N–CH=CH–CHO (as measured by UV-absorbance changes). The generation of 95.1 and 97.1, or 69.1 *m/z* was observed in the irradiation time of 5 or 30 min. MS spectra for anionic compounds: the peak at 95.1 *m/z* was identified as the intermediate of $C_4H_3OHN_2$. The intermediates from OP underwent further photooxidation to generate smaller peaks at 95.1 and 97.1 *m/z*. The chemical structures of NH=N–CH=CH–CH=CHOH (97.1 *m/z*) and CH_2=CH–CH=CHOH (69.1 *m/z*) indicated cleavage of the C–N bond, and their formation led to easy evolution of N_2 gas. LC-MSD analysis for positive EPA data (cationic compounds) of MP corroborated the photooxidation mechanism. The photodegradation of MP during the initial stage (10 min) yield peaks at 71.1 *m/z* (NH_2–CH=N–CHO), 101.2 *m/z* (NH_2–CH=CH–CH=N–CH_2OH) and 113.1 *m/z* (CHO–N–CH=CH–CH=N–CHO). The decrease of the 71.1 *m/z* peak only was examined after UV-illumination for 15 min. Possibly the photooxidation of MP proceeded via many oxidation steps. Evidence for intermediates during the photooxidation of PP was obtained from MS spectra of cationic compounds (positive EPA data). Irradiation for 10 min led to an increase in new peaks at 65.1, 88.1 and 113.1 *m/z*. The peaks were assigned to CH_3CH_2COOH (65.1 *m/z*), CH_2OH–CH=N–CHO (88.1 *m/z*) and CHO–N=CH–CH=N–CHO (113.1 *m/z*). The many other peaks in the LC-MSD measurements were supposed to be from amines, aldehydes and carboxyl derivatives.

4. Photodegradation mechanisms

The photodecomposition mechanism of OP is tentatively proposed in Scheme 1. In the initial step, the N=N fragment in OP was adsorbed onto the TiO_2 surface, and the C^3 and C^6 atoms were preferentially attacked by $^{\bullet}$OH radicals. Otherwise, direct oxidation of OP proceeded by photooxidation by holes in the TiO_2 photocatalyst. The two cationic intermediates formed by addition of –OH to the carbon of the N–C fragment. Afterwards opening of the ring of OP was caused by UV-illumination. HOC–N=N–CH=CH–CHO and NH=N–CH=CH–CH=CHOH intermediates were generated in the next step. The latter reaction was slow compared to the former. The intermediate CHO–N=N–CH=CH–CHO was mineralized to N_2 gas and carbon-containing intermediates. The residual intermediates with carbon atoms were photodecomposed by $^{\bullet}$OH radicals, and the succeeding reaction led to the generation of CH_3CH_2COOH, CH_3COOH, HCOOH and HCHO. The decomposition of the NH=N–CH=CH–CH=CHOH intermediate led to N_2 gas and the CH_2=CH–CH=CHOH intermediate. The inter-

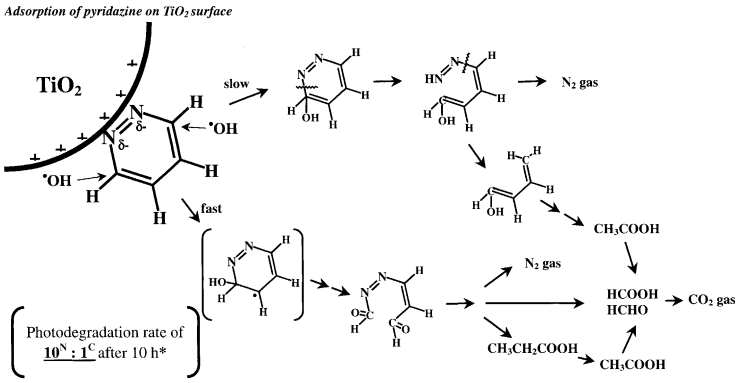

Scheme 1. Proposed photodegradation mechanism of OP (∗: one atom of nitrogen:one atom of carbon).

mediates containing carbon was mineralized to CO_2 gas via CH_3COOH, HCOOH and HCHO. Subsequently, N_2 gas was easily formed by photodegradation of the intermediates. The final photomineralization product (CO_2 gas) resulted from photodegradation of the intermediates. The photomineralization of the nitrogen atoms was carried out more simply than that of the carbon atoms in OP.

Making use of both the analytical data and the calculation results, the simple photodecomposition mechanism of MP is proposed in Scheme 2. After adsorption of the N=C–N fragment to the positive TiO_2 surface, the initial photodegradation of MP took place at the TiO_2/H_2O interface and •OH radicals attacked the C^5 position from opposite sides. Competitive direct oxidation to MO was caused by holes in the TiO_2. The photodegradation mechanism was organized into the following three processes. Step (I) was the generation of N-containing intermediates of NH_2–CH=N–CHO or CH_3COOH after the attack of •OH radicals. Acetic acid was mineralized to CO_2 gas by further photodegradation. The photodecomposition mechanism of NH_2–CH=N–CHO continued with the formation of two NH_2–CHO intermediates by scission of the C=N bond. The two steps (II) and (III) generated heterorings having a $•C^6$ or $•N^1$ radical. However, the formation of these heteroring radical-containing structures was in principle impossible. The (II) way led to the formation of CHO–N–CH=CH–CH=N–CHO by ring opening, and scission of the C=N bond caused evolution of CO_2 gas via carboxy and aldehyde derivative intermediates. The photodegradation of NH_2–CHO was via the same mechanism as step (I). In step (III), the NH_2–CH=CH–CH=N–CH_2OH intermediate was initially supposed to form the (CHO–N=CH–CH=CHO) intermediate and the NH_4^+ ion. Evolution of CO_2 gas began when UV-irradiation was further continued. The rapid initiation in the degradation of MP occurred more competitively in three pathways rather than that of OP and PP.

The photodecomposition mechanism of PP is illustrated in Scheme 3. Two nitrogen atoms were adsorbed on the TiO_2 surface. The two initial photooxidations were enhanced by preferential attack of •OH radicals at the carbon atoms, and direct oxidation of PP was by photooxidation caused by holes in TiO_2. These reactions led to the generation of CHO–N=CH–CH=N–CHO. The intermediates NH_2–CHO and $HOCH_2$–CH=N–CHO were generated from

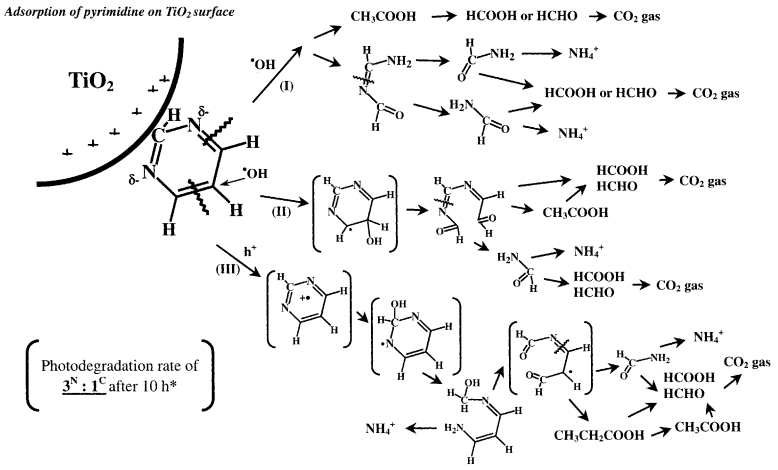

Scheme 2. Proposed photodegradation mechanism of MP (∗: one atom of nitrogen:one atom of carbon).

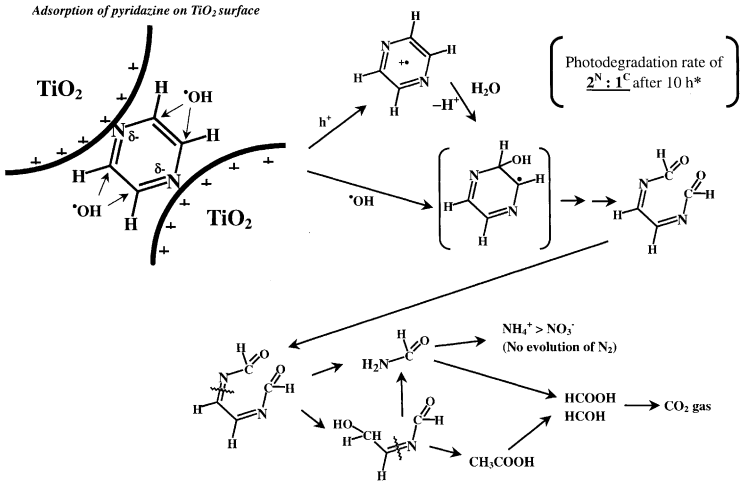

Scheme 3. Proposed photodegradation mechanism of PP (∗: one atom of nitrogen:one atom of carbon).

scission of the N=C fragment. The evolution of NH_4^+ ions and/or NO_3^- ions, and CO_2 gas in the photodegradation of NH_2–CHO were easy reactions: the carbon atoms of the $HOCH_2$–CH=N–CHO intermediate were photodecomposed to CHCOOH and HCHO, via NH_2–CHO and CH_3COOH. The final process was the evolution of NH_4^+ or NO_3^- ions, and CO_2 gas. The ease of ion formation followed the order $NH_4^+ \gg NO_3^-$.

The rates of photooxidation of the nitrogen atom and carbon atoms followed the order OP $\gg$ PP $>$ MP, which was consistent with the presence of a N=N fragment and the richer frontier electron density on the surface-adjacent side of the N atom position in the chemical structure.

5. Conclusion

In the photocatalytic degradation of nitrogen-containing cyclic compounds, the N=N moiety was converted into N_2 gas, and the N–C moiety was degraded into NH_4^+ ions and/or NO_3^- ions ($NH_4^+ \gg NO_3^-$). The calculation of frontier electron density and point charge suggests the site of initial adsorption on the TiO_2 surface and the site of initial photooxidation by attacking $^\bullet$OH radicals. The complicated photooxidation followed the order MP $\gg$ OP $>$ PP. The photodegradation mechanisms were deduced by comparison of the experimental data with the MO calculations.

Acknowledgements

This research was financially supported by Grants-in-aid for Scientific Research from the Japanese Ministry of Education, Culture, Sports, Science and Technology (No. 10640569). The authors also thank N. Watanabe and M. Mukae for their technical assistance.

References

[1] C.K. Gratzel, M. Jirousek, M. Gratzel, J. Mol. Catal. 39 (1987) 347.
[2] C.K. Gratzel, M. Jirousek, M. Gratzel, J. Mol. Catal. 60 (1990) 375.
[3] K. Harada, T. Hisanaga, K. Tanaka, New J. Chem. 11 (1987) 597.
[4] K.W. Krosley, D.M. Collard, J. Adamson, M.A. Fox, J. Photochem. Photobiol. A: Chem. 69 (1993) 357.
[5] M. Kerzhentsev, C. Guillard, J.M. Hemnann, P. Pichat, in: D.F. Ollis, H. Al-Ekabi (Eds.), Photocatalytic Purification and Treatment of Water and Air, Elsevier, New York, 1993, pp. 601–606.
[6] H. Hidaka, J. Zhao, Y. Satoh, K. Nohara, E. Pelizzetti, N. Serpone, J. Mol. Cata1. 88 (1994) 239.
[7] H. Hidaka, H. Kubota, M. Gratzel, N. Serpone, E. Pelizzetti, Nouv. J. Chim. 9 (1985) 67.
[8] E. Pelizzetti, M. Barbeni, E. Paramauro, N. Serpone, E. Borgarello, M.A. Jamieson, H. Hidaka, Chim. Ind. (Milan) 67 (1985) 623.
[9] F. Sabin, T. Turk, A. Vogler, J. Photochem. Photobiol. A: Chem. 63 (1992) 99.
[10] A.L. Pruden, D.F. Ollis, Environ. Sci. Technol. 17 (1983) 628.
[11] A.L. Pruden, D.F. Ollis, J. Catal. 82 (1983) 418.
[12] T. Nguyen, D.F. Ollis, J. Phys. Chem. 88 (1984) 3386.
[13] C.S. Turchi, D.F. Ollis, J. Catal. 122 (1990) 187.
[14] R.W. Matthews, Water Res. 20 (1986) 569.
[15] G.K.-C. Low, S.R. McEvoy, R.W. Matthews, Environ. Sci. Technol. 25 (1991) 460.
[16] G.K.-C. Low, S.R. McEvoy, R.W. Matthews, Chemosphere 19 (1989) 1611.
[17] E. Pelizzetti, C. Minero, P. Piccinini, M. Vincenti, Coord. Chem. Rev. 125 (1993) 183.
[18] C. Maillard, C. Guillard, P. Pichat, Chemosphere 24 (1992) 1085.
[19] C. Maillard, C. Guillard, P. Pichat, New J. Chem. 18 (1994) 941.
[20] S. Horikoshi, N. Serpone, S. Yoshizawa, J. Knowland, H. Hidaka, J. Photochem. Photobiol. A: Chem. 120 (1998) 63.
[21] S.D. Kahn, C.F. Pau, L.E. Overman, W.J. Hehre, J. Am. Chem. Soc. 108 (1986) 7381.
[22] H. Kaczmarek, A. Kaminska, M. Swiatek, J.F. Rabek, Die Ang. Makromol. Chem. 261 (1998) 109.